Catalysis Letters Vol. 107, Nos. 3–4, March 2006 (© 2006)
DOI: 10.1007/s10562-005-0003-9

Effect of sol–gel synthesis on physical and chemical properties of V/SiO_2 and V/MgO catalysts

Yu-Chuan Lin and Keith L. Hohn*

Department of Chemical Engineering, Kansas State University, Manhattan, KS, 66506, USA

Received 15 September 2005; accepted 2 December 2005

Catalytic properties of supported vanadium oxide catalysts are highly dependent on surface vanadia configuration and the nature of the support. In this study, the effects of using the same supports (silica and magnesia) from two different preparation procedures on the catalytic properties in methanol partial oxidation and on the vanadium surface structures were investigated. Both types of catalysts were prepared by the incipient-wetness method and characterized using BET, Raman spectroscopy, UV–Vis and H_2-TPR to determine the structures of vanadium on the supports' surface. Both aerogel-prepared V/SiO_2 and V/MgO catalysts were more active than conventionally prepared samples in methanol partial oxidation. These differences in catalytic results are attributed to the configurations of active phase. It was also found that small vanadium phases were more active in methanol partial oxidation than larger phases.

KEY WORDS: methanol partial oxidation; vanadium; vanadium pentoxide; aerogel; silica; magnesia.

1. Introduction

Supported vanadium oxide catalysts have attracted numerous studies in the last decade [1–11]. Catalytic properties of vanadium oxide catalysts are highly dependant on catalytic surface configurations, identities of active sites, and interactions between vanadyl species and oxide supports [12–15]. In recent years, researchers have paid much more attention on the effect of oxide supports, which were long believed to be inert in the catalytic reaction. They have also reported that by modifying the oxide supports with other oxides possessing different acid–base properties, the reactivity of catalyst can be enhanced [7,12,15–17].

In recent years, there has been an explosion of work in nanotechnology, where materials with features on the order of nanometers are prepared. Sol–gel techniques have been used to synthesize metal oxides with crystal sizes of only nanometers [18], and these metal oxides have been found to have different chemical and catalytic properties than conventional metal oxides [19]. For example, the surface hydroxyls on sol–gel prepared MgO have been found to be less acidic than on conventional MgO [19]. Also sol–gel prepared MgO was found to have a much higher adsorption capacity per nanometer of surface area for acid gases for low partial pressures of those gases [20]. Our laboratory has previously reported that butene selectivity during oxidative dehydrogenation of butane was higher when nanocrystalline MgO was used as the support, and it was hypothesized that differences in support acid–base properties might have played a role [4].

This literature suggests that nanocrystalline metal oxides may lead to different catalytic properties than conventional supports, but there is a lack of understanding for how the nanocrystalline metal oxides affect catalysis. One possibility is that the support changes the acid–base properties or redox properties of the resulting supported catalyst. This would be analogous to how different metal oxides (i.e. MgO versus TiO_2) lead to different chemical properties that affect catalyst activity. Another possibility is that the increased surface area of the nanocrystalline supports leads to differences in the supported phase or phases. This paper studies how the use of two aerogel-prepared (AP) metal oxides (SiO_2 and MgO) as supports for vanadium affects the vanadium surface phases and the chemical properties of the catalysts. Methanol partial oxidation is used as a probe of acid/base and redox properties of the catalysts [21], while H_2-TPR is used to evaluate the reducibility of the catalysts. Several techniques are used to characterize the physical properties of the catalysts (BET, Raman spectroscopy, and UV–Vis spectroscopy).

This paper also looks at how turnover frequency in methanol oxidation varies as a function of vanadium weight loading. There are conflicting reports in the literature. Wachs and co-workers reported a slight initial increase in turnover frequency with increasing vanadium loading on various metal oxide supports followed by a decrease [16]. However, they also reported no trend in turnover frequency with weight loading, citing results where TiO_2 was used as the support [7]. Bell and co-workers recently reported that vanadium surface

---

*To whom correspondence should be addressed.

density played an important role in oxidative dehydrogenation, where vanadium phases containing bridging vanadate groups were more active than monovanadate structures [22]. Therefore, important mechanistic information can be obtained by understanding how turnover frequency varies with vanadium weight loading. Using sol–gel prepared SiO_2 and MgO offers a means for investigating this question because their high surface areas should allow more vanadium to be loaded without forming bulk phases.

2. Experimental section

2.1. Catalyst preparation

Two types of SiO_2 and MgO were applied in this study: conventionally prepared (CP) and aerogel prepared (AP) silicon and magnesium oxides. CP SiO_2 was purchased from Degussa (Aerosoil-380, $S_{BET} = 367\ m^2/g$), and pretreated with water to allow easy handling. CP MgO was prepared by pretreating commercially purchased MgO (Aldrich, 99 + %) in boiling water overnight with stirring. After cooling and filtering, the paste of magnesium hydroxide was dried in an oven at 120 °C for 2 h and then calcined at 500 °C under vacuum overnight.

AP SiO_2 was formed by a sol–gel process combined with supercritical drying in a bench-top autoclave (Parr Model 4843). The details of sol–gel process, developed by Rolison and coworkers, are reported elsewhere [18]. The gel-like product was dried over a 4-h period in an autoclave heated from room temperature to 265 °C.

For AP MgO, 5 g of magnesium ribbons (Alfa Aesar, 99.8 + %) was reacted with 200 mL methanol under nitrogen for 2 h. The resulting solution was mixed with 200 mL toluene and then 4 mL deionized water was slowly added. This mixture was stirred overnight and transferred into an autoclave, where it was dried with a hypercritical drying process [19]. The remaining white magnesium hydroxide powder was calcined at 500 °C under vacuum overnight. [4]

All supports were calcined at 500 °C under vacuum for 4 h and stored in beakers under an ambient atmosphere for a few days. Vanadium was then introduced onto each support by the incipient-wetness method, following the procedure described by Wachs and coworkers [14].

2.2. Catalyst characterization

The surface areas of all samples were measured by a Quantachrome NOVA 1200 instrument. Before each run, approximately 0.1 g of catalyst was degassed at 300 °C for 30 min. Six-point BET surface areas were calculated from the nitrogen adsorption isotherms.

Raman spectra of hydrated samples were obtained by a Chromex Raman 2000 instrument in 200–2000 cm^{-1} wavelength range with 785 nm laser beam. Ground samples were packed within plastic cuvettes and placed inside a cuvette holder (Quantum Northwest TLC 50) for spectra collections.

Temperature-programmed reduction of hydrogen was measured in an Altamira AMI-200 system. 0.2 g samples were loaded in a quartz U-tube reactor and treated at 550 °C for 1 h in pure O_2 to fully oxidize the samples. After cooling, the temperature was ramped from 50 °C to 850 °C at a constant rate of 5 °C/min in a flow of 5% H_2 in Ar. H_2 consumption was monitored using a thermal conductivity detector (TCD).

UV–Vis spectra were acquired by a Varian-Cary 500 Scan UV–Vis NIR spectrophotometer with an integrating sphere attachment in the 1.5–6.2 eV photon energy range. The absorption spectra were acquired with Teflon powder as a reference. The adsorption edge energy was measured by a least-squares fit of a line through a low energy edge of an absorption spectrum [22,23].

2.3. Catalytic reactivity testing

Methanol partial oxidation was applied as a chemical probe of both CP- and AP- V/SiO_2 and V/MgO catalysts. Experiments were performed in an 11-mm i.d. vertical quartz tube reactor placed inside a cylindrical furnace. Approximately 60 mg samples were loaded between plugs of quartz wool, which resulted in a bed length of about 0.2 cm. A K-type thermocouple was placed at the bottom of the catalyst bed. Product gasses were sent to a gas chromatograph (SRI 8610) that used MolSieve 5A and Haysep T columns to separate the products. Two kinds of detectors, FID and TCD, were equipped to analyze the products during the reaction. Products detected include oxygen, nitrogen, carbon monoxide, carbon dioxide, water, formaldehyde, dimethyl ether, methanol, methyl formate, and dimethoxy methane.

Both oxygen (99.0%) and nitrogen (97.0 + %) were obtained from Linweld. Methanol (99.9%) was obtained from Fisher. Methanol was introduced into the system by a syringe pump (New Era NE-500) with a 0.01 mL/min injection rate. Gas flows of oxygen and nitrogen were regulated by mass flow controllers (Brooks Instrument, 5850E) and blended with methanol vapor to achieve a 13/81/6 (mole%) mixture. The total flow rate was around 100 standard cubic centimeters per minute (sccm).

All catalysts were pelletized, crushed, and sieved into 20–40 mesh particles. Internal and external mass transfer resistances were examined by changing particle size and gas flow rate, and were found to be negligible. Before each run, samples were pretreated at 450 °C for 30 min in a stream of oxygen and nitrogen. Catalytic results were acquired at 250 °C for V/SiO_2 catalysts and 150 °C for V/MgO catalysts, beginning 20 min after injection of methanol through the system. Blank runs were performed in the reactor with packed quartz wool without any detectable conversion of methanol.

For all data reported, the carbon and hydrogen mass balances closed within 10% error and most within 5%. For each sample, three to five trials were run. These multiple trials were used to estimate 95% confidence intervals for catalytic activity, selectivity and turnover frequency (TOF). Activity was calculated from conversion: the number of moles of methanol converted per hour per gram catalyst (mol/h×g), noted as Ac. The selectivity (%) of product X_i was calculated as 100×(number of moles methanol converted to product X_i)/(total number of moles of methanol converted). Turnover frequency (s^{-1}), defined as the moles of methanol converted per surface vanadium atom per second [7], was found by dividing activity by the number of active sites per gram of catalyst. The number of active sites was calculated from the number of vanadium atoms, found from the nominal weight loading.

3. Results

3.1. Physical properties

Tables 1 and 2 present the surface areas, calculated surface vanadia densities and UV–Vis absorption edge energies of all AP and CP V/SiO$_2$ and V/MgO catalysts. With increasing vanadium loading, the surfaces areas of all samples generally decrease. Surface areas of all AP catalysts are at least twice as high as CP catalysts. This increased surface area resulted in much lower vanadium surface densities for AP catalysts for the same weight loadings.

Table 3 lists tshe colors of hydrated and dehydrated AP and CP V/SiO$_2$ catalysts with various loadings. For hydrated samples, colors were recorded under ambient condition; for dehydrated samples, observations were obtained after purging with pure oxygen at 450 °C for 30 min. The colors of silica and V$_2$O$_5$ crystals were white and orange, respectively, for hydrated and dehydrated samples. With increasing vanadium content, the colors of AP and CP samples became darker. CP samples became orange at high weight loadings, while AP samples did not.

Previous studies found that hydrated monovanadate species and V$_2$O$_5$ phases on a silica surface were yellowish and orange in color, separately. When samples were dehydrated at elevated temperatures, the monovanadate species become white while the orange color was maintained by vanadium pentoxide phases [14]. This suggests that samples with darker colors contain more crystalline V$_2$O$_5$.

Table 1

Surface areas, surface compositions and UV–Visible absorption edge energies of AP and CP V/SiO$_2$ catalysts

wt%	AP V/SiO$_2$			CP V/SiO$_2$		
	Surface area (m^2/g)	Surface density (VO$_x$/nm^2)	Absorption edge energy (eV)	Surface area (m^2/g)	Surface density (VO$_x$/nm^2)	Absorption edge energy(eV)
0	760.9	0		270.6	0	
0.5	772.1	0.04	2.20	268.6	0.12	2.11
1	742.3	0.09	2.15	260.5	0.25	2.08
2	716.6	0.18	2.10	268.1	0.48	2.00
3	618.1	0.31	2.05	262.1	0.74	2.01
5	564.3	0.56	2.07	244.1	1.29	1.91
7	551.1	0.79	2.03	240.6	1.80	1.89
10	566.0	1.06	2.03	206.4	2.92	1.89

Table 2

Surface areas, surface compositions and UV–Visible absorption edge energies of AP and CP V/MgO catalysts

wt%	AP V/SiO$_2$			CP V/SiO$_2$		
	Surface area (m^2/g)	Surface density (VO$_x$/nm^2)	Absorption edge energy (eV)	Surface area (m^2/g)	Surface density (VO$_x$/nm^2)	Absorption edge energy(eV)
0	285.0	0		126.1	0	
5	263.4	1.2	2.75	124.2	2.5	2.75
10	266.2	2.3	2.70	114.2	5.3	2.65
15	252.0	3.4	2.68	88.3	9.8	2.68
20	224.7	4.9	2.75	88.9	12.4	2.65
25	206.3	6.4	2.64	76.6	17.3	2.59
30	156.3	9.8	2.65	70.3	21.7	2.49

Table 3
Colors of hydrated and dehydrated AP and CP V/SiO$_2$ catalysts

wt%	AP V/SiO$_2$		CP V/SiO$_2$	
	Hydrated color	Dehydrated color	Hydrated color	Dehydrated color
0	White	White	White	White
1	Light yellow	White	Light yellow	White
3	Light yellow	White	Yellow	Light yellow
5	Yellow	Light yellow	Orange	Yellow
10	Yellow	Light yellow	Orange	Orange

3.2. Raman spectroscopy

No clear V = O signal was observed for AP or CP V/SiO$_2$ catalysts at any weight loading. This may be due to interference from the silica support, or because hydrated surface vanadyl groups are difficult to detect.

Figure 1 presents the Raman spectra of AP and CP V/MgO catalysts with vanadium weight loadings of 0%, 5%, 10%, 20%, 25%, and 30%. Reference phases, including $Mg_3(VO_4)_2$, $Mg_2V_2O_7$ and V_2O_5, were also collected. Consistent with previous studies, $Mg_3(VO_4)_2$ shows a clear Raman peak at 864 cm^{-1} [24–26], whereas $Mg_2V_2O_7$ gives Raman peaks at 947 and 901 cm^{-1} [26,27]. None of these peaks are apparent between 0% to 10%. At vanadium weight loadings of 20% and above, both AP and CP V/MgO catalysts exhibit a strong peak at ~860 cm^{-1}, which can be ascribed to the V–O bond stretching vibration in $Mg_3(VO_4)_2$. The characteristic peaks of $Mg_2V_2O_7$ were not present in any AP V/MgO catalysts; in contrast, a sharp peak at 951 cm^{-1} assigned to magnesium pyrovanadate has been found for 25% and 30% CP V/MgO. A small but clear peak at ~1010 cm^{-1} was observed for 20%, 25%, and 30% AP V/MgO catalysts, but its assignment is not clear.

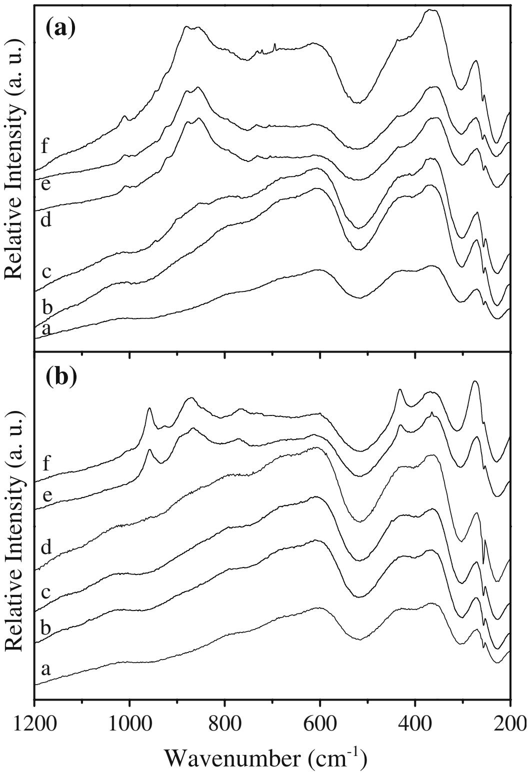

Figure 1. Raman spectra for hydrated (A) AP V/MgO and (B) CP V/MgO with (a) 0%, (b) 5%, (c) 10%, (d) 20%, (e) 25% and (f) 30% vanadia weight loadings in the 200–1200 cm^{-1} range.

3.3. H_2 Temperature-programmed reduction

3.3.1. V/SiO$_2$

TPR profiles for 1%, 3%, 5%, and 10% vanadia loadings on AP and CP silica supports showed only one reduction peak. The peak where the H_2 consumption is maximum, noted as T_{max}, increased with increased loading and was similar for AP and CP V/SiO$_2$ catalysts. The T_{max} for 1%, 3%, 5% and 10% AP V/SiO$_2$ were located at 507, 537, 538, and 576 °C, while 1%, 3%, 5% and 10% CP V/SiO$_2$ had T_{max} at 508, 519, 540, and 580 °C. One broad peak may enclose multiple peaks from several surface vanadyl phases [16]. According to previous work, crystalline V_2O_5 on silica possesses the highest T_{max} of any vanadyl species [7,27,28]. Thus, at higher vanadia loadings, there may be more V_2O_5 on the silica surface.

3.3.2. V/MgO

For 10%, 20%, and 30% vanadia on AP and CP magnesia supports only one reduction peak was observed. The T_{max} of 10%, 20% and 30% AP V/MgO are at 661, 676 and 708 °C, while 10%, 20% and 30% CP V/MgO had T_{max} at 651, 698 and 748 °C. The asymmetric shape (shoulder) of each peak on the low-temperature side suggested that there were at least two types of vanadia phases [29,30].

A linear trend between vanadia loading and hydrogen consumption was observed for both AP and CP V/SiO$_2$ and V/MgO samples. Moreover, the H_2 consumptions for AP and CP samples were within 10% for the same vanadium weight loading. This suggests that the actual vanadium loadings are close to the nominal values.

3.4. Diffuse reflectance UV–Vis

Figure 2 shows the UV–Vis spectra of 1%, 5% and 10% AP and CP V/SiO$_2$. V_2O_5, shown as a reference,

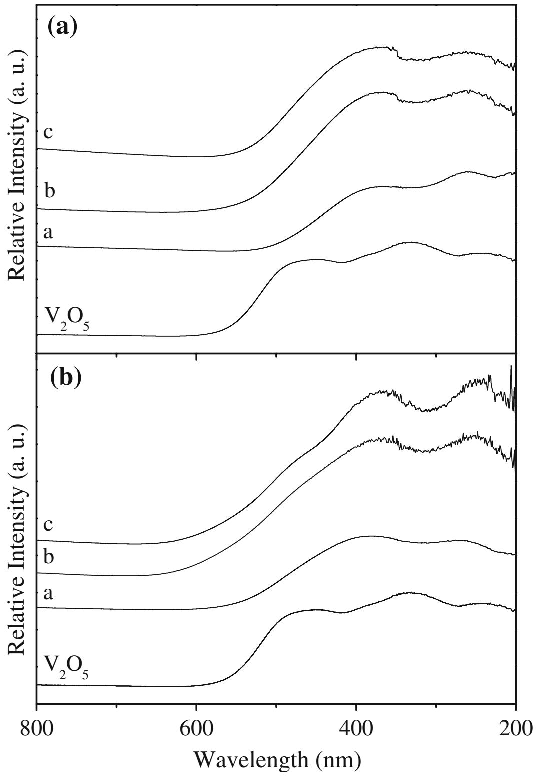

Figure 2. UV–Visible spectra for (A) AP V/MgO and (B) CP V/MgO with (a) 1%, (b) 5% and (c) 10% vanadia weight loadings.

possesses three absorption bands at 500–400, 400–300 and 300–200 nm. For AP samples, none of the absorption bands from V_2O_5 was found. On the contrary, higher loading CP samples, including 5% and 10%, exhibit a shoulder near 500 nm. This may indicate the presence of V_2O_5. Tables 1 and 2 show the dependence of UV–Vis absorption edge energy on vanadia loading for all catalysts. A recent article discussing the relation between the absorption edge energy and size of surface oxide domains noted that the bandgap energy of a real system decreases as the domain size increases [31]. Therefore, the decreasing absorption edge energies with increasing vanadia contents shown in tables 1 and 2 imply that the sizes of the two-dimensional active oxide domains grow [23]. Moreover, AP catalysts possess higher edge energies than CP catalysts for both V/SiO$_2$ and V/MgO at almost all loadings. This suggests that surface vanadia phases on AP supports were smaller than those on CP supports.

3.5. *Catalytic studies*

Methanol partial oxidation is a useful probe reaction for comparing chemical properties of different supports [7]. For instance, the types of catalytic sites (redox, acidic and basic) can be probed by observing the products formed [21].

3.5.1. *V/SiO$_2$*

Formaldehyde selectivity at 3% vanadium weight loadings and higher were about 83% for both AP and CP V/SiO$_2$ catalysts but AP samples generally had higher conversions. For weight loadings lower than 2%, CP samples gave ~70% formaldehyde selectivity while AP samples had 60% at roughly the same conversion. The selectivity difference can be attributed to the silica support, rather than to differences in vanadium structure, since isolated monovanadate species are expected on both AP and CP V/SiO$_2$ due to the low vanadium surface densities. Comparing activity on a vanadium surface density basis, as is done in figure 3, shows that both AP and CP catalysts have nearly the same activity at all surface densities.

3.5.2. *V/MgO*

The selectivities to formaldehyde were about 77% for both series, while carbon oxides, dimethyl ether, methyl formate and methyal were all less than 10%. On a wt% basis, AP V/MgO was more active at 10% weight loadings and higher. However, when TOF is comparted as a function of vanadia surface density, as shown in figure 4, both catalysts have roughly the same TOF. As was seen for V/SiO$_2$ catalysts, TOF of both AP and CP V/MgO decreased with increased vanadium loadings.

4. Discussion

4.1. *Catalyst structure*

4.1.1. *V/SiO$_2$*

At low vanadium weight loading (< 3%) on both supports vanadium is likely found as monomeric vanadyl groups. This is indicated by the white color of the dehydrated V/SiO$_2$. The vanadium surface density for these weight loadings (< 0.74 V atoms/nm^2) is

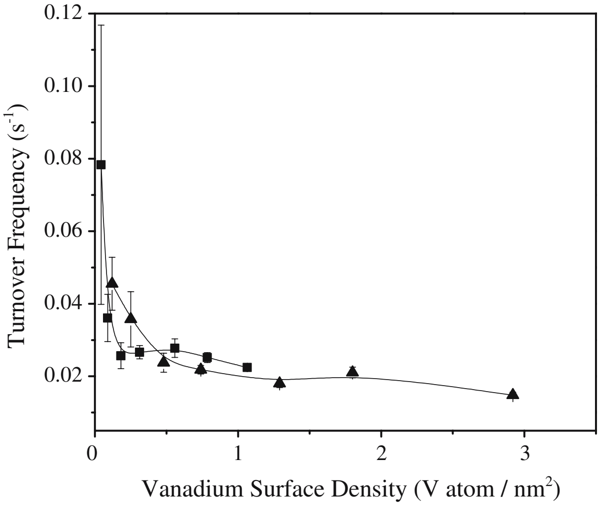

Figure 3. Turnover frequency (s^{-1}) for AP V/SiO$_2$ (■) and CP V/SiO$_2$ (▲) with different vanadia surface densities.

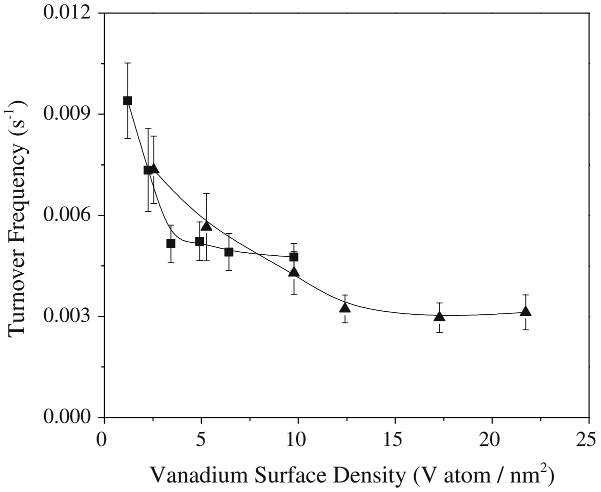

Figure 4. Turnover frequency (s^{-1}) for AP V/MgO (■) and CP V/MgO (▲) with different vanadia surface densities.

sufficiently low that isolative monovanadate species would be expected [14].

At loadings 3% and higher, V_2O_5 is formed on CP V/SiO_2, but not on AP V/SiO_2. For CP V/SiO_2, an orange color, characteristic of V_2O_5, was noted for 5% and higher hydrated catalysts and 10% dehydrated catalysts. In addition, the UV–Vis spectra showed a shoulder for 5% and 10% CP samples close to the index band of V_2O_5. No AP samples were orange, and no shoulder was noted in the UV–Vis spectra.

It is to be expected that V_2O_5 would be increasingly present as the vanadium weight loading increases. Gao and co-workers have reported that ~2.6 V atoms/nm^2 is the maximum coverage of isolated monovanadate species on conventional silica [14]. As seen in table 1, a weight loading of 10% CP V/SiO_2 gives a surface density of 2.92 V atoms/nm^2, so V_2O_5 would be expected. This is not the case for all AP V/SiO_2 samples, which have vanadium surface densities far less than 2.6 V atoms/nm^2.

4.1.2. V/MgO

For AP V/MgO, only $Mg_3(VO_4)_2$ was detected for weight loadings 10% and higher. The absence of $Mg_2V_2O_7$ peak for AP V/MgO was attributed to the V/Mg atomic ratio on the surface of magnesia support. According to previous studies, with an increase of vanadia contents, $Mg_3(VO_4)_2$ was the first component detected, then both $Mg_3(VO_4)_2$ and $Mg_2V_2O_7$ were seen [32,33]. Therefore, AP MgO, which has nearly three times larger surface area than CP MgO, can maintain small domains of $Mg_3(VO_4)_2$ with no or an undetectable amount of $Mg_2V_2O_7$ at higher vanadia loadings.

The coexistence of $Mg_3(VO_4)_2$ and $Mg_2V_2O_7$ on CP V/MgO at 25% and above implied that with increasing of vanadia loading, the domains of magnesium vanadates grew and/or aggregated, leading to formation of high V/Mg atomic ratio compounds, e.g. magnesium pyrovanadate.

4.2. Catalyst selectivity and reactivity

4.2.1. V/SiO_2

Catalytic activity for AP and CP V/SiO_2 were nearly the same for weight loadings less than 3%. However, statistically significant differences were noted at 3% and higher. There are two possible explanations for the differences. The first is that the interaction between the supported vanadium phases and the support are different when AP and CP silica are used. Previous work has indicated that different supports give orders of magnitude differences in TOF and this difference has been attributed to the reducibility of the metal–oxygen–vanadium bond [7,16]. Another possibility is that different surface vanadium phases are formed on the two supports that have different intrinsic activities.

If there are differences in the interaction between the supported vanadium phases and the support, differences in TOF would be observed for all weight loadings. This is not the case: TOF of AP and CP catalysts are very close at almost all weight loadings. In addition, this hypothesis would suggest that the TPR results for AP and CP catalysts would be quite different, since the reducibility of the Si–O–V bond is thought to be critical for determining catalyst activity [7,34,35]. This is also not the case: the $T_{\max}$ of AP and CP catalysts are within 5 °C of each other for all weight loadings, with the exception of 3% samples where a 18 °C difference is found.

It is, therefore, hypothesized that the activity difference is due to differences in the vanadium phases present at high weight loadings on AP and CP catalysts. This would be consistent with the observation that TOF is essentially the same for AP and CP at weight loadings less than 3%: only monovanadate should be present on both catalysts. It is hypothesized that CP catalysts have more V_2O_5 present at the same weight than AP catalysts, and this increased amount of V_2O_5 lowers the activity of CP catalysts relative to AP catalysts.

This hypothesis assumes that V_2O_5 is less active than monovanadate species. This is counter to the trend that Wachs and Deo suggest [7], but in agreement with results reported by Koranne *et al.* [36] who found that monovanadate on V/SiO_2 catalysts was more active than bulk V_2O_5 in the partial oxidation of methane.

Figure 3 shows a decrease in TOF as the V_2O_5 weight percent is increased on both AP and CP V/SiO_2. This is consistent with aggregated phases being less active than isolated monovanadate species. It was noted that the activity of 30% CP V/SiO_2 (which is covered by bulk V_2O_5) was $2.2 \times 10^{-2}\ s^{-1}$, which is in good agreement with that reported in the literature for bulk V_2O_5 [37]. This value is less than that found for low weight loading catalysts (<3%) where only monovanadate is expected, again suggesting that V_2O_5 is less active than isolated monovanadate.

4.2.2. V/MgO

AP V/MgO catalysts were more active than CP V/MgO at 20% loading and higher. However, if the TOF are compared based an vanadium surface density, AP V/MgO exhibited equivalent TOF as CP samples. This may imply that with the identical surface density, there is no difference between surface magnesium vanadate groups on AP and CP MgO, which resulted in the close TOF values. The decrease of TOF also indicated that the intrinsic activity of V/MgO catalyst was controlled by surface vanadia phases: the larger the magnesium vanadate groups, the less active the catalyst was. This suggests that small domains of vanadyl groups on magnesia support are more active than magnesium vanadate clusters.

4.2.3. Effect of sol–gel prepared supports

The results suggest that the primary difference between sol–gel prepared supports and other supports is that nanocrystalline supports are better able to disperse the supported vanadium phases. This leads to isolated vanadyl groups in the case of V/SiO$_2$ and formation of orthovanadate rather than pyrovanadate in the case of V/MgO. This led to higher activity than for conventional supports at higher weight loadings for either SiO$_2$ or MgO because large vanadium domains seem to be less active than small domains. Use of a nanocrystalline support does not appear to change the acid/base nature or the redox properties of the supported vanadium catalysts: product selectivities were nearly identical when either support morphology was used.

4.2.4. Dependence of turnover frequency on vanadium surface density

TOF decreased with increasing vanadium surface density for all catalysts. This decrease was significant for low weight loadings of vanadium, while turnover frequency was nearly constant for high weight loadings. Since isolated vanadyl groups are likely present at lower weight loadings, while polymeric or bulk phases are present at higher weight loadings, this trend suggests that isolated vanadyl groups are more active for methanol oxidation.

For this to be the case, isolated vanadyl groups should be more active in the rate-determining step in methanol oxidation, which is the decomposition of methoxy [38]. In this step, methoxy decomposes to gas phase formaldehyde and surface hydroxyl. As a result of this step, the active site is reduced; therefore the reducibility of the active site would be expected to play a role in catalyst activity. A number of investigators have found a correlation between catalyst activity and surface reducibility [7,39]. As seen in our H_2-TPR results, the $T_{\max}$ of reduction progressively increases with increasing vanadium weight loading, so the decrease in turnover frequency occurs simultaneously with a decrease in surface reducibility.

The decreased surface reducibility can be explained by the different vanadium phases present for different weight loadings. The UV–Vis results demonstrate a decrease in absorption edge energy with increasing weight loading. This decrease is likely caused by larger vanadium domains [24]. For larger domains, the V–O–M (where M is the support metal) bonds are replaced by V–O–V bonds. We propose that these bonds are less reducible than V–O–M bonds, leading to lower activity. The turnover frequency tends to level off at higher weight loadings for all catalysts. This can be explained by noting that at high weight loadings polymeric vanadium phases have become dominant, so even as the total vanadium weight loading goes up, the type of phase does not change.

5. Conclusions

The catalytic differences between AP and CP V/SiO$_2$ and V/MgO catalysts are explained by the configurations of active phases on supports. The larger surface areas of AP silica and magnesia are able to support smaller active domains than conventional supports. This difference is hypothesized to be responsible for the higher TOF noted for AP catalysts at equivalent weight loadings. Small vanadium domains were more active than larger domains for methanol oxidation since TOF decreased as vanadium surface density increased.

Acknowledgments

The authors express their appreciation to Professor Israel E. Wachs and Edward Lee of Lehigh University for research advice. The authors also acknowledge Professor Russell C. Middaugh and Nick Harn of University of Kansas for assistance in acquiring all Raman spectra. The authors also thank Dr. Kenneth J. Klabunde and Johanna Häggström of Kansas State University for the collection of all UV–Vis spectra. This work was supported by DOE EPSCOR Grant DE-FG02-01ER45896.

References

[1] M.A. Chaar, D. Patel, M.C. Kung and H.H. Kung, J. Catal. 105 (1987) 483.
[2] D. SiewHew Sam, V. Soenen and J.C. Volta, J. Catal. 123 (1990) 417.
[3] P.M. Michalakos, M.C. Kung, I. Jahan and H.H. Kung, J. Catal. 140 (1993) 226.
[4] R. Vidal-Michel and K.L. Hohn, J. Catal. 221 (2004) 127.
[5] M. Inomata, A. Miyamoto, T. Ui, K. Kobayashi Y. Murakami, Ind. Eng. Chem. Prod. Res. Dev. 21 (1982) 424.

[6] M.S. Wainwright and N.R. Foster, Catal. Rev.-Sci. Eng. 19 (1979) 211.
[7] G. Deo and I.E. Wachs, J. Catal. 146 (1994) 323.
[8] S. Irusta, L.M. Cornaglia, E.E. Miro and E.A. Lombardo, J. Catal. 156 (1995) 157.
[9] Q. Sun, J.M. Jehng, H. Hu, R.G. Herman, I.E. Wachs K. Klier, J. Catal. 165 (1997) 91.
[10] G.L. Rice and S.L. Scott, J. Mol. Catal. A: Chem. 125 (1997) 73.
[11] M.A. Banares, X. Gao, J.L.G. Fierro and I.E. Wachs, Stud. Surf. Sci. Catal. 110 (1997) 295.
[12] G.T. Went, S.T. Oyama and A.T. Bell, J. Phys. Chem. 94 (1990) 4240.
[13] P. Forzatti, E. Tronconi, A.S. Elmi and G. Busca, Appl. Catal. A 157 (1997) 387.
[14] X. Gao, S.R. Bare, J.L.G. Fierro, M.A. Banares and I.E. Wachs, J. Phys. Chem. B 102 (1998) 5653.
[15] L.J. Burcham and I.E. Wachs, Catal. Today 49 (1999) 467.
[16] G. Deo, I.E. Wachs and J. Haber, Cri. Rev. Surf. Chem. 4 (1994) 141.
[17] X. Gao and I.E. Wachs, Top. Catal 18 (2002) 243.
[18] M.L. Anderson, C.A. Morris, R.M. Stroud, C.I. Merzbacher and D.R. Rolison, Langmuir 15 (1999) 674.
[19] K.J. Klabunde, J. Stark, O. Koper, C. Mohs, D.G. Park S. Decker, Y. Jiang, I. Lagadic and D. Zhang, J. Phys. Chem. 100 (1996) 12142.
[20] I.V. Mishakov, A.F. Bedilo, R.M. Richards, V.V. Chesnokov, A.M. Volodin, V.I. Zaikovskii, R.A. Buyanov and K.J. Klabunde, J. Catal. 206 (2002) 40.
[21] J.M. Tatibouët, Appl. Catal. A 148 (1997) 213.
[22] K. Chen, A.T. Bell and E. Iglesia, J. Catal. 209 (2002) 35.
[23] D.G. Barton, M. Shtein, R.D. Wilson, S.L. Soled and E. Iglesia, J. Phys. Chem. B 103 (1999) 630.
[24] C. Pak, A.T. Bell and T.D. Tilley, J. Catal. 206 (2002) 49.
[25] J. Hanuza, B. Jezowska-Trzebiatowska and W. Oganowski, J. Mol. Catal. 29 (1985) 109.
[26] G. Busca, G. Ricchiardi, D.S.H. Sam and J.-C. Volta, J. Chem. Soc., Faraday Trans. 90 (1994) 1161.
[27] F. Roozeboom, M.C. Mittelmeijer-Hazeleger, J.A. Moulijn J. Medema, V.H.J. De Beer and P.J. Gellings, J. Phys. Chem. 84 (1980) 2783.
[28] M.M. Koranne, J.G. Goodwin Jr. and G. Marcelin, J. Catal. 148 (1994) 369.
[29] T. Blasco, J.M. López Nieto, A. Dejoz and M.I. Vazquez, J. Catal. 157 (1995) 271.
[30] F. Arena, F. Frusteri and A. Parmaliana, Appl. Catal. A. 176 (1999) 189.
[31] R.S. Weber, J. Catal. 151 (1995) 470.
[32] T. Blasco and J.M. López Nieto, Appl. Catal. A 157 (1997) 117.
[33] X. Gao, P. Ruiz, Q. Xin, X. Guo and B. Delmon, J. Catal. 148 (1994) 56.
[34] A.J. van Hengstum, J.G. van Ommen, H. Bosch and P.J. Gellings, Proc. 8th Internat. Cong. Catal., Vo1.4, Dechema, Frankfurt-am-Main, Vol. 4, 1984, p. 297.
[35] J. Haber, A. Kozolowski and R. Kozolowski, J. Catal. 102 (1986) 52.
[36] M.M. Koranne, J.G. Goodwin Jr. and G. Marcelin, J. Catal. 148 (1994) 388.
[37] G. Deo and I.E. Wachs, J. Catal. 129 (1991) 307.
[38] C.J. Machiels and A.W. Sleight, J. Catal. 76 (1982) 238.
[39] F. Roozeboom, P.D. Cordingley and P.J. Gellings, J. Catal. 68 (1981) 464.
[40] C. Tellez, M. Abon, J.A. Dalmon, C. Mirodatos and J. Santamaria, J. Catal. 195 (2000) 113.